

Geophysical Research Letters



RESEARCH LETTER

10.1029/2021GL094235

Key Points:

- Juno performed 4 years of observations of the Jupiter polar cyclones. We discuss implications for their stability and vertical structure
- The cyclones have similar intrinsic oscillation frequencies, and perturbations seem to propagate from one cyclone to the closer one
- Cyclones are extremely stable, individually and as a whole; they slowly spin and the South one is twice as fast as the North one

Supporting Information:

Supporting Information may be found in the online version of this article.

Correspondence to:

A. Mura,
alessandro.mura@inaf.it

Citation:

Mura, A., Adriani, A., Bracco, A., Moriconi, M. L., Grassi, D., Plainaki, C., et al. (2021). Oscillations and stability of the Jupiter polar cyclones. *Geophysical Research Letters*, 48, e2021GL094235. <https://doi.org/10.1029/2021GL094235>


Received 10 MAY 2021

Accepted 25 JUN 2021

© 2021. The Authors.

This is an open access article under the terms of the [Creative Commons Attribution License](https://creativecommons.org/licenses/by/4.0/), which permits use, distribution and reproduction in any medium, provided the original work is properly cited.

Oscillations and Stability of the Jupiter Polar Cyclones

A. Mura¹ , A. Adriani¹ , A. Bracco² , M. L. Moriconi³ , D. Grassi¹ , C. Plainaki⁴ , A. Ingersoll⁵ , S. Bolton⁶, R. Sordini¹, F. Altieri¹ , A. Ciarravano³ , A. Cicchetti¹ , B. M. Dinelli³ , G. Filacchione¹ , A. Migliorini¹ , R. Noschese¹ , G. Piccioni¹ , P. Scarica¹, G. Sindoni⁴, S. Stefani¹ , F. Tosi¹ , and D. Turrini¹ 

¹INAF - Istituto di Astrofisica e Planetologia Spaziali, Roma, Italy, ²Georgia Institute of Technology, Atlanta, GA, USA, ³CNR - Istituto di Scienze dell'Atmosfera e del Clima, Bologna and Roma, Italy, ⁴Agenzia Spaziale Italiana, Roma, Italy, ⁵California Institute of Technology, Pasadena, CA, USA, ⁶Southwest Research Institute, San Antonio, TX, USA

Abstract Juno discovered the circumpolar cyclones polygons on Jupiter in 2017. Fundamental questions regarding Jovian cyclogenesis concern the formation mechanism and whether these cyclones are deep or shallow. Recent data by Juno/JIRAM infrared camera show that any change is an extremely unlikely event on an annual scale. Only once, in 2019, a sixth cyclone joined the pentagonal structure in the South, but it disappeared after 2 months without merging with the pre-existing cyclones; disappearance or creation of stable cyclones has never been observed. Additionally, the rotation speeds of the north and south polygons as a whole are not compatible with the shallow hypothesis; both structures drift at a much smaller rate than the typical scale velocities on Jupiter surface, and differ at the two poles. Cyclones oscillate around what may seem like equilibrium positions, and these oscillations tend to propagate from one cyclone to another. These oscillations have almost equal timescales, and here we investigate the possible implications of such similarity.

Plain Language Summary Juno/JIRAM performed four year of observations of the circumpolar structures at Jupiter. We investigate three major properties of these structures: they spin slowly, but at different rates, the South one being twice as fast as the North one; both structures as a whole, and the 15 singular cyclones are extremely stable; the cyclones have similar intrinsic oscillation frequencies, and perturbations seem to propagate from one cyclone to the closer one.

1. Introduction

Juno is a NASA mission to study the origin and evolution of Jupiter, in orbit since August 2016 (Bolton, Adriani, et al., 2017, Bolton, Lunine, et al., 2017). In February 2017 it discovered the existence of the Jupiter circumpolar cyclones, thanks to the observation by the Jovian InfraRed Auroral Mapper, JIRAM (Adriani et al., 2017, 2018) and JunoCam (Hansen et al., 2014). JIRAM, in particular, has been monitoring the evolution of these structures since then; the North Pole is occupied by a polar cyclone surrounded by eight circumpolar cyclones (CPCs) while the South Pole is characterized by five cyclones surrounding a polar cyclone. Circumpolar cyclones have approximately the same size as their relative polar cyclone, and southern cyclones are larger than northern ones.

JIRAM is an imager and a spectrometer in the 2–5 μm infrared range, devoted to the study of the atmosphere and aurorae of Jupiter. The study of Jupiter's atmosphere is performed by both imaging in the *M* band (a filter of the imager channel covering the spectral range from ~ 4.6 to ~ 5.1 μm) and spectral observation in the 2–5 μm range. Both the imager and the spectrometer have an angular resolution of 237 μrad and can operate simultaneously. In this study, we use images in the *M* band. These are images of the ammonia clouds shielding the thermal emission of the planet at different viewing angles. Regions free of clouds will appear “hotter” (light red color), that is, with higher radiance (Adriani et al., 2017, 2018, 2020). The polar cyclones have thick clouds (dark red color) that obstruct most of the view of the deeper atmosphere (see Figure 1).

JIRAM can take only one image and one spectrum for each spin of Juno (~ 30 s). Over the poles, the observational strategy of JIRAM is to acquire a certain number of contiguous images in a sequence, covering a strip of the Jovian surface, and then restart another sequence to point to an adjacent strip, so as to cover most of the region within the 80° latitude, where the cyclones are located. Consequently, when possible, most of

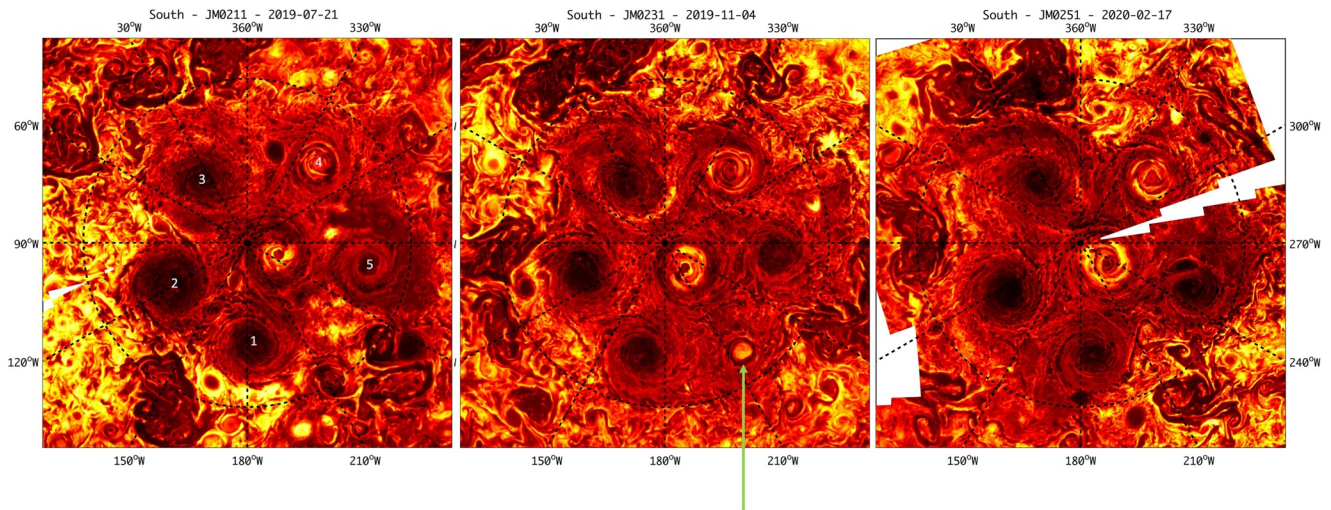


Figure 1. Maps of M band radiance in the South Pole during three different orbits, covering the circumpolar structures. From left to right: orbit 21 (July 2019), orbit 23 (Nov. 2019) and orbit 25 (Feb. 2020). The sixth cyclone, indicated by a green arrow in the middle panel, appears in orbit 22 (Aug. 2019), forms an almost perfect hexagon in orbit 23 (Nov. 2019), starts to vanish in orbit 24 and disappears completely in orbit 25 (Feb. 2020) (see Supplementary Material for orbits 22 and 24). The radiance goes from 0.02 to $0.8 \text{ W m}^{-2} \text{ sr}^{-1}$ and the color scale is logarithmic. In the left panel, blue numbers identifying the cyclones are also plotted.

the polar surface is covered by two or more consecutive images of JIRAM. In this case, we always use the image with higher spatial resolution. Since the acquisition always occurs over a time interval of one hour or less it can reasonably be assumed that the position of the center of the cyclones has not changed in this time frame. All the single images used in this work have been corrected for the emission angle with a law similar to Beer's law (see Methods). However, given the nature of this study, the correction of the radiance is not critical. The data is given in unit of band radiance, $\text{W sr}^{-1} \text{ m}^{-2}$.

Because of the precession of the orbit of Juno and the orientation of its spin plane, the observation of the north cyclones is usually possible when the spacecraft passes over the North Pole, at a very low altitude. As a result, it is difficult to have a global coverage of the north structure, and it will be so until mid 2022. However, while the coverage of the North Pole cyclones has been partial, the observations of the South Pole continued at regular intervals, and here we report the time period between orbit four (PJ4, Feb. 2017) and 30 (PJ30, Nov. 2020). Over these four year the pentagonal structure did not change substantially, only occasional perturbations have been observed. From the partial observations of the North Pole, we can also conclude that the octagonal structure is still present. Small anticyclonic structures within the CPCs have been often observed both at the North Pole and at the South Pole, and anticyclonic structures with radii smaller than 1,000 km are present at all times, as discussed in Adriani et al. (2020). Maximum wind speeds are observed at about 1,000 km from the centers of the cyclones, and vary between 100 and 55 m/s, depending on the specific vortex considered (Grassi et al., 2018); the analysis demonstrated also that lower velocities characterize the smaller anticyclonic vortices. In this study, however, we do not discuss the anticyclones, but we focus on the secular (long term, i.e., the four years in this study) variability of the location of the much larger cyclones.

Since the discovery of the polar cyclone structures at Jupiter (Adriani et al., 2018) is relatively new, few modeling studies have attempted explaining their stability and even fewer their genesis. In most cases, the models follow those of Saturn polar patterns, with two main line of investigation under the assumption that the structures are “shallow” and extend to few tens of bars into the Jovian atmosphere, or “deep” and reach well into tens of thousands of bars. In the first case, quasi-geostrophic and shallow water models have been adopted to understand the stability of the observed patterns. Reinaud (2019) and Reinaud and Dritschel (2019), for example, have shown that a quasi-geostrophic vortex subject to an azimuthal instability at a given wave number m may develop into an array of m same-sign vortices. Depending on m the array can be stable, and the likelihood increases if a vortex of the same sign is included at center of it. Their work, however, does not account for the change in Coriolis parameter as the latitude varies, the so-called

beta-effect, which is responsible for the drift of cyclonic eddies toward the Pole, and may affect stability. Li et al. (2020) included the beta-effect and seeded a given number of (shallow) cyclones in a shallow water model. The simulated cyclones are pushed poleward by the planet rotation and group into regular polygonal patterns that are stable whether the shallow layer hosting them is not too thin or too deep and only if each cyclone is shielded by an anticyclonic ring of vorticity. In these simulations the entrance of a new cyclone into an existing polygonal structure induces a semi-permanent change in the structure. In laboratory experiments, vortex clusters comparable to the ones observed on Jupiter can emerge spontaneously in a three-dimensional shallow water setting (Boury et al., 2021) in response to wave-like perturbations, but a sloped bottom bathymetry such as a conical mountain.

“Deep” models, on the other hand, generally adopt rotating Boussinesq thermal convection equations (e.g., Heimpel et al., 2005; 2016). They can reproduce deep convective plumes, but current computational resources limit the Rayleigh number they can achieve and therefore the realism of the simulated turbulence. The Rayleigh number, or Ra , is the ratio of two time scales, that for diffusive thermal transport and that for convective thermal transport at a given speed, and was estimated for Jupiter to be greater than 10^{12} (Manneville & Olson, 1996). One of the most recent applications of rotating thermal convective models, presented in Garcia et al. (2020), for example, achieved only $Ra \sim 10^5$. It showed that deep convection can occur on Jupiter or Saturn poles, but did not reproduce the details of the observed structures or their stability. Cai et al. (2021) therefore seeded a deep convective model with Jupiter polar cyclones to match the observations, concluding that deep convective, packed, long-lived cyclones can be stable on Jupiter poles due to the large Coriolis parameter. Yadav and Bloxham (2020) partially overcame the computational limitations adopting the simpler anelastic approximation (Lantz & Fan, 1999) in deep convection simulations of Saturn on a spherical shell. They produced self-consistently the hexagonal flow pattern and the single cyclone observed at its poles. An interesting outcome of these numerical integrations is that they also reproduce the slow rotation rate of the Saturn hexagonal pattern, a detail not captured by shallow models where the wind field (or the imposed external forcing) sets the rotation speed.

To test the validity and accuracy of the two main classes of models, shallow and deep, there are at least two basic physical quantities that can be checked at Jupiter poles: the winds and their relationship with the cyclones, and the secular variations of the polygonal structures. The winds can be calculated by using multiple images of the same regions at short time scale (Grassi et al., 2018); from the wind field, it is possible to calculate the (shallow) vorticity distribution they map onto and infer how it should move. For example, the model by Li et al. (2020) requires a mean, stable field of anti-cyclonic winds in between cyclones to ensure their shielding and therefore their stability. The secular, long-term variability of the polygons, which includes the motion of their centers, the oscillation, the observation of merging events, the disappearing or appearing of new cyclones or anticyclones, is the other helpful quantity which is the object of this study.

2. Data

In Table 1 we present the sequence of all the observations of the South Pole from 2017 to today, while Table 2 summarizes the available observations of the North Pole. Juno’s orbit lasts about 53 days; therefore, this is the minimum time interval between two successive observations reported here. As mentioned, the coverage of the North Pole is less complete than that of the South Pole due to Juno’s orbit inclination and precession of periapsis (it moved from 6°N at orbit 4 to 26°N at orbit 30, getting closer and closer to the North Pole). Overall the spatial resolution at the North Pole is higher, but the coverage is limited.

We used the NAIF-SPICE software (Acton, 1996) for each geometric calibration, as done in all other studies involving JIRAM data, and the uncertainty about the geometry reconstruction of JIRAM images is equal to, or less than, one pixel. After the geometric calibration, the spatial resolution at the reference level of 1 bar is variable and ranges approximately from 15 to 60 km, depending on the position of Juno. The position of the center of the cyclones cannot be determined with automatic recognition software (the morphology of cyclones changes and the “eye” is not completely visible occasionally) and therefore it has been identified manually, for all cyclones and for all orbits in which there was coverage of a given cyclone (see Supplementary Material). In the Supplementary Material section, we show the images, superimposed on the estimated position of the center of the cyclones. The variability of cyclone sizes is not covered in this study. For a study

Table 1
Summary of South Pole Observations

PJ	Type	Date	Lat 1 (°S)	Lat 2 (°S)	Lat 3 (°S)	Lat 4 (°S)	Lat 5 (°S)	Lat SP (°S)	Lon 1 (W°)	Lon 2 (W°)	Lon 3 (W°)	Lon 4 (W°)	Lon 5 (W°)	Lon SP (W°)
4	GRAV	12/11/2016	83.7	84.3	85.0	84.1	83.2	88.6	157.1	94.3	13.4	298.8	229.7	211.3
5	MWR	02/02/2017	83.0	84.3				87.8	160.9	103.4				203.1
6	MWRTilt	03/27/2017	83.1	84.7	85.5	84.1	82.3	87.6	160.3	102.2	11.9	289.0	234.4	213.9
8	MWR	07/11/2017	83.6	85.2	85.4	83.4	82.4	87.8	160.4	93.1	12.4	302.3	248.1	238.1
9	GRAV	09/01/2017	83.8	84.8	84.9	83.4	82.9	88.5	167.9	97.6	12.4	305.1	250.3	239.1
11	GRAV	12/16/2017	83.2	84.1	84.7	84.3	83.1	88.5	167.8	106.6	28.5	304.1	240.2	215.0
13	-30/+20	04/01/2018	83.1	84.7	85.8	84.1	82.5	88.1	173.6	114.1	27.4	301.5	245.8	222.3
14	GRAV	05/24/2018	83.5	85.1	85.2	83.7	82.6	87.9	178.2	111.8	17.3	303.0	245.5	232.8
15	GRAV	07/16/2018	84.4	85.0	84.7	83.4	82.6	88.0	174.2	104.0	18.7	306.2	238.9	250.8
17	-30/+20	10/29/2018	83.5	84.5	84.9	83.9	82.8	88.3	170.5	107.6	29.9	309.4	251.4	225.8
18	GRAV	12/21/2018	83.3	84.4	85.5	84.3	82.7	87.8	170.9	112.1	32.7	316.1	260.1	224.4
19	GRAV	02/12/2019	83.1	84.5	85.5	84.0	82.8	87.7	176.4	119.5	31.1	316.2	259.5	230.3
20	MWRXtk	04/06/2019	83.4	84.6	85.1	83.9	82.9	88.0	183.7	119.6	35.4	317.8	256.6	242.3
21	-30/+5	05/29/2019	84.0	84.8	85.4	83.5	82.5	87.9	182.7	118.9	33.3	318.0	259.4	250.5
22	GRAV	07/21/2019	83.8	84.8	85.2	83.8	82.8	88.2	176.9	116.9	31.2	319.4	264.0	245.4
23	GRAV	09/12/2019	83.0	84.6	85.8	83.9	83.1	88.0	168.0	110.6	32.8	318.2	263.5	224.3
24	GRAV	11/03/2019	82.8	84.3	85.5	84.3	83.3	87.9	175.2	117.6	33.5	316.5	259.0	217.5
25	GRAV	12/26/2019	83.1	84.6	85.5	84.1	82.7	88.0	186.3	123.0	35.7	312.6	247.0	234.8
26	GRAV	02/17/2020	83.7	84.8	85.8	83.7		87.3	185.9	126.2	33.1	318.1		254.4
27	GRAV	04/10/2020	84.1	84.8		83.3	82.2	87.3	190.8	119.7		323.9	252.4	269.5
28	GRAV	06/02/2020	84.2	85.3	84.9	83.2	82.8	87.9	190.8	124.9	31.2	323.1	250.2	270.2
30	GRAV	09/16/2020	83.8	84.4	85.0	83.9	83.0	88.6	185.0	122.3	47.8	327.3	255.5	258.7

Note. GRAV stands for Gravity orbit, when the antenna is pointing to Earth; in the other cases the s/c spin axis is tilted to allow better coverage of the polar regions. Central cyclone close to the South pole is named “SP”.

Table 2
Summary of North Pole Observations

PJ	Lat 1 (°N)	Lat 2 (°N)	Lat 3 (°N)	Lat 4 (°N)	Lat 5 (°N)	Lat 6 (°N)	Lat 7 (°N)	Lat 8 (°N)	Lat NP (°N)	Lon 1 (°W)	Lon 2 (°W)	Lon 3 (°W)	Lon 4 (°W)	Lon 5 (°W)	Lon 6 (°W)	Lon 7 (°W)	Lon 8 (°W)	Lon NP (°W)
4	82.9	83.8	82.0	83.2	82.9	83.2	82.3	83.5	89.6	1.4	50.7	95.3	137.6	183.4	227.6	269.9	314.8	230.4
5					83.1	83.2	81.8							179.7	227.3	269.7		
6	83.2	83.7	82.0	83.2	82.8	83.1	81.9	83.3	89.9	359.0	50.2	95.5	136.6	183.6	226.5	271.8	311.8	193.0
9	82.6		83.1	83.4	83.2	83.8	82.1	83.4		359.3		89.8	135.0	179.9	227.5	268.0	312.6	
10			82.3				82.1		89.5			93.7				271.1		107.8
14		83.2			83.2	84.2					53.0			194.0	244.6			
16	82.8		82.7	82.7		83.9	81.6		89.4	6.4		100.4	147.6		244.2	285.1		118.2
24		83.1				83.8			90.0		59.6				235.5			211.0
26	83.2	83.4	82.8	82.5	82.7				89.8	7.0	56.3	102.0	143.6	190.4				240.5
28	83.2	83.1	82.3							9.0	58.2	104.2						

Note. See Table 1 for date and orbit type.
Abbreviation: Polar cyclone, NP.

of the systematic differences between the North Pole and the South Pole, we refer to the article by Adriani et al., 2017. The analysis also revealed the presence of many wavy structures hovering over some parts of the cyclones; such topic is described in details in the paper by Moriconi et al. (2020).

3. Results

One of the most important characteristics regarding the stability and evolution of the polar cyclones on Jupiter is their average life span. No changes in the number of cyclones or shape of the polar structures were observed in four years. The only significant event was the entry, in the southern structure, of a sixth cyclone that occupied the space between two cyclones at about 210°W for about 6 months. This event is showed in Figure 1 where the maps of the radiance for the South pole are shown. These images are composites of several image sequences acquired by JIRAM and plotted on geographic coordinates.

Specifically, in July 2019, two south CPCs (CPC1 and CPC5 as they are referred in Table 1) began to move apart, leaving an empty region in between (longitudes from 180 to 270W), where a sixth cyclone, smaller than the ones in the existing structure, appeared in September 2019. The then-six CPCs occupied the vertices of a hexagon for a couple of months, until December 2019, when the new CPC6 disappeared without merging with CPC1 or CPC5. It must be noted that a careful analysis of the available sequences (see Supplementary Material) suggests that this event was not the joining/exiting of an external cyclone moving poleward/equatorward, but rather the fast formation/disappearance of a new, small cyclone in the space freed by the moving apart of the two cyclones. This event and its characteristics should be accounted for in the cyclogenesis theory.

Apart from this event, no other significant modification of the CPC structures has been recorded in four years. It is therefore impossible to estimate the average life of the cyclones. The 2019 event (the appearance of a sixth temporary CPC in the South) is indeed not representative because, as noted, that cyclone was different from the other five in many aspects, among others being smaller and with higher radiance. However, a simple calculation can be made taking into account all the cyclones present at both poles (6 at the South and 9 at the North). Assuming that these 15 cyclones have a similar lifetime τ , the probability ($e^{-t/\tau}$) that they all are alive after 4 years reaches 5% (a common threshold for the null hypothesis) only when τ exceeds 20 years. We therefore suggest that the average lifetime of a single cyclone is very long. However, this simple calculation assumes that the CPCs are independent in terms of lifetime. This may not be the case (we already know that they are not independent in terms of positions) and therefore the possible disappearance of one cyclone could affect the stability of all the others in the same group, which is likely.

In addition to the fluctuations of the cyclones, occasionally large anticyclones can form in between the CPCs. For example, and as described in Adriani et al., (2020) a large one was located at about 87°N latitude from at least February 2017 (the first JIRAM observation during PJ4), and lasted no less than one year. Its size was about 2,000 km in diameter, grew slowly over time, and during its lifetime oscillated in the region between the polar cyclone and the circumpolar cyclones. Unfortunately, because of the above-mentioned limitations in coverage, the subsequent evolution of this structure could not be monitored continuously, but we know that it either disappeared or exited the CPCs structure.

A convenient way to investigate the group motion and the relative motion of the CPCs is by plotting their longitude as a function of time, as done in Figure 2. The first noticeable feature is a general westward drift, already discussed in Tabataba-Vakili et al. (2020). Here, however, we can quantify the angular velocity with better precision, since we have more data over a much longer time period. If we fit the longitudes with simple slopes, we obtain the values reported in Table 3. The overall westward drift is $7.5 \pm 0.7^\circ$ per year in the South Pole. In the north, where data are fewer the long-term drift is more uncertain and estimated to be $3 \pm 3^\circ$ per year. The uncertainty is mostly determined by the evolution of CPC7 and CPC8, which have the shortest time coverage (2 years). Removing them from the calculation of the average secular drift leads to a value of $3 \pm 1^\circ$ per year. Hence, we can conclude that the average drift is substantially different among the two Poles and slower in the North. Finally, we note that the central cyclone in the south polygon is spinning around the South Pole too.

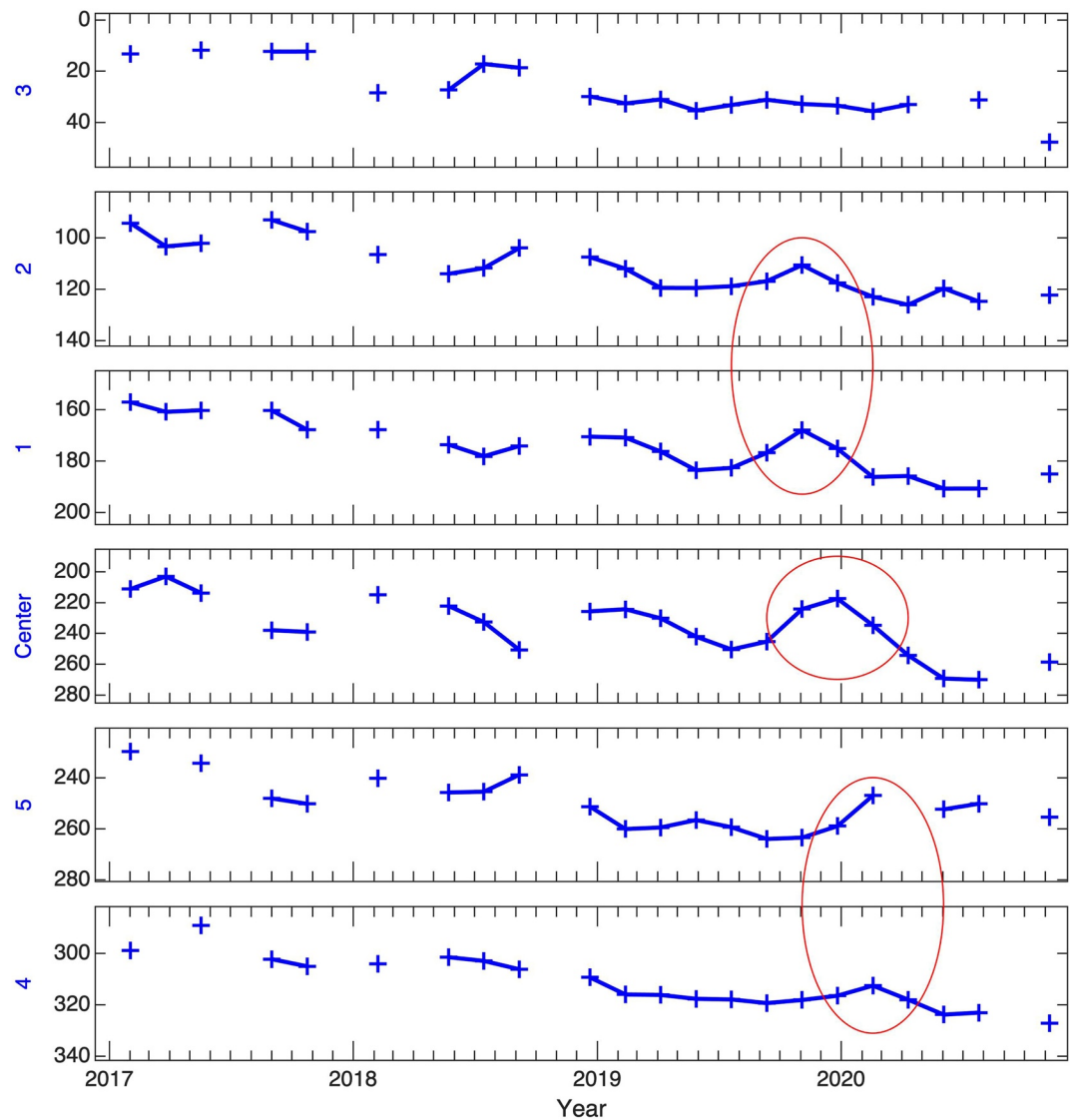


Figure 2. Longitude of cyclones as a function of time. Each cyclone has a separate plot, the red ovals indicate the oscillation analyzed in the text. Longitudes are West, and axes are downward.

Another interesting feature emerges from the analysis of Figure 2: there are fairly regular oscillations that are transmitted from cyclone to cyclone. The best observed example is an oscillation that begins shortly at the end of 2019 in the pair of Southern CPCs 1 and 2, propagates to the central cyclone and then to CPCs 4 and 5 (red ovals in Figure 2 indicates the event). It is worth noting that in this period CPCs 1 and 5, that are usually close to each other, were separated by the “intruder” (sixth cyclone event in late 2019), and likely because of this the perturbation could not be transmitted directly from 1 to 5. Other fluctuations may have occurred in different periods, when the time coverage was less optimal. All the oscillations visible in Figure 2 occur on a time scale of about 4–6 months.

4. Discussion and Conclusions

Our work provides observational evidence of three important characteristics of the CPCs of Jupiter: the cyclones in the structures are long-living and stable; the CPCs rotate very slowly; the cyclones are subjected to oscillations that propagate from one to the other.

Table 3
Secular Drift Velocities for the Cyclones (Westward), and Average Drift

South (°/year)		North (°/year)	
CPC 1	8.0	CPC 1	2.6
CPC 2	7.9	CPC 2	2.4
CPC 3	7.3	CPC 3	3.1
CPC 4	8.0	CPC 4	2.9
CPC 5	6.4	CPC 5	3.3
		CPC 6	5.2
		CPC 7	8.0
		CPC 8	-2.7
Average	7.5 ± 0.7	Average	3 ± 3*

Note. CPCs 7 and 8 have the shortest time coverage, and if we exclude them from the calculation of the average we obtain 3 ± 1°/year.

Abbreviation: circumpolar cyclone, CPC

While the stability may be achieved independently of the depth of the cyclones in both shallow and deep models (Cai et al., 2021; Li et al., 2020; Reinaud & Dritschel, 2019; Yadav & Bloxham, 2020), the fact that in both hemispheres the average angular velocity of the polar structures is extremely low—it takes between 50 and 100 years to complete a rotation around the pole—points to a deep nature. The instabilities within and around the cyclones, on the other hand, are reminiscent of those found in the well-mixed surface boundary layer in the ocean (Adriani et al., 2020; Lapeyre & Klein, 2006) and signal the presence of an explicit stratification in the upper portion of the polar atmosphere. The CPCs rotation is indeed much lower than any typical scale velocity on Jupiter, such as that of zonal winds that would be (co)responsible for forcing them whenever the cyclones extended only to a shallow portion of the atmosphere. Their speed is also much lower than that of the outermost structures (small cyclones and anticyclones), observed immediately equatorward of the CPCs.

“Deep” models suggest that vortices occurring in gas giants form by deep planetary turbulent convection and that configurations as those observed on Jupiter’s poles can be stable (Cai et al., 2021). Heimpel et al. (2016)

and Yadav et al. (2020) report that anticyclones and cyclones forming through convective driving display a prevalence of clockwise or anticlockwise rotation according to the vorticity of the local wind shear, but their rotation and genesis may also be impacted by the dynamo layer underneath the atmospheric hydrodynamic layer. Additionally, Heimpel et al. (2016) have proposed a correlation between a stronger convective forcing and a higher number of polar cyclones.

We stress that the “2019 intruder” showed characteristics closer to those of the more external cyclones, which tend to be smaller, move faster and form and dissolve frequently. Its formation/dissolution in 2019 could be justified under the hypothesis of a shallow, well-mixed outer layer, where the dynamics and their timescales may be reasonably approximated by forced shallow water, quasi-geostrophic or surface quasi-geostrophic equations.

Regarding the oscillations, it is reasonable to think that they occur around a hypothetical position of equilibrium and are governed by phenomena akin to those of an elastic force on an object with inertia acting on all 5 cyclones at the South Pole (and presumably also on those at the North). The laboratory model proposed by Boury et al. (2021) may indicate a viable mechanism for the oscillations.

Finally, the different angular velocity and different number of cyclones observed at the two Poles are suggestive of slightly different Rayleigh number regimes, possibly linked to different stratification profiles.

In conclusions, we presented four years of observations of circumpolar structures at Jupiter, performed by the JIRAM instrument aboard Juno. We focused on the main properties of secular variability of these structures. The two CPC structures and the 15 cyclones that form them are extremely stable, with an estimated lifetime of at least 20 years. The cyclones have similar intrinsic oscillation frequencies, and perturbations seem to propagate from one cyclone to the nearest one. The average spin rate of the polygonal structures is measured, and it is about twice as fast in the south than in the north. All these properties together suggest that the 15 major cyclones differ in size, lifespan, stability, and secular properties from the smaller ones that are observed equatorward of the CPCs, and that the CPCs are similar among themselves. The slow rotation of the CPC structures—slow compared to the surface wind speed—and their stability are indicative of a convective origin, deep-rooted in the Jovian atmosphere.

The properties we identified are crucial for testing hypotheses regarding the cyclogenesis, structure and role of the polar cyclones in the overall circulation and elemental distribution of Jupiter’s atmosphere. While no numerical experiment performed so far can satisfactorily explain all these characteristics, the analysis presented allows for refining the modeling framework.

Data Availability Statement

JIRAM data used in this study is publicly available on the Planetary Data System (<http://pds.nasa.gov>) and can be downloaded from <http://atmos.nmsu.edu:8080/pds>. The individual datasets are available at http://atmos.nmsu.edu/PDS/data/jnojr_XXXX, where XXXX is 1,001, 1,002, or 1,003 for EDR (Experiment Data Record; raw data) and 2001, 2002, or 2003 for RDR (Reduced Data Record; calibrated data) volumes.

Acknowledgments

This work was supported by the Italian Space Agency through ASI-INAF contract I/010/10/0 and 2014-050-R.O. The JIRAM instrument was developed by Leonardo at the Officine Galileo - Campi Bisenzio site. Open Access Funding provided by Istituto nazionale di astrofisica within the CRUI-CARE Agreement.

References

- Acton, C. H. (1996). Ancillary data services of NASA's Navigation and Ancillary Information Facility, Planet. *Space Sci*, 44, 65–70. [https://doi.org/10.1016/0032-0633\(95\)00107-7](https://doi.org/10.1016/0032-0633(95)00107-7)
- Adriani, A., Bracco, A., Grassi, D., Moriconi, M. L., Mura, A., Orton, G., et al. (2020). Two-year observations of the Jupiter polar regions by JIRAM on board Juno. *Journal of Geophysical Research*, 125(Issue 6), e2019JE006098. June 2020. <https://doi.org/10.1029/2019JE006098>
- Adriani, A., Filacchione, G., Di Iorio, T., Turrini, D., Noschese, R., Cicchetti, A., et al. (2017). JIRAM, the Jovian infrared auroral mapper. *Space Science Reviews*, 213, 393–446. <https://doi.org/10.1007/s11214-014-0094-y>
- Adriani, A., Mura, A., Orton, G. S., Hansen, C., Altieri, F., Moriconi, M. L., et al. (2018). Clusters of cyclones encircling Jupiter's poles. *Nature*, 555, 216–219. <https://doi.org/10.1038/nature25491>
- Bolton, S. J., Adriani, A., Adumitroaie, V., Allison, M., Anderson, J., Atreya, S., et al. (2017). Jupiter's interior and deep atmosphere: The initial pole-to-pole passes with the Juno spacecraft. *Science*, 356(6340), 821–825. <https://doi.org/10.1126/science.aal2108>
- Bolton, S. J., Lunine, J., Stevenson, D., Connerney, J. E. P., Levin, S., Owen, T. C., et al. (2017). The Juno Mission. *Space Science Reviews*, 213, 5–37. <https://doi.org/10.1007/s11214-017-0429-6>
- Boury, S., Sibgatullin, I., Ermanyuk, E., Ermanyuka, N., Odier, P., Joubaud, S., et al. (2021). Vortex cluster arising from an axisymmetric inertial wave attractor. ArXiv:2009.06928v1 [physics.flu-dyn].
- Cai, T., Chan, K. L., & Mayr, H. G. (2021). Deep, closely packed, long-lived cyclones on Jupiter's poles. *The Planetary Science Journal*, 281, 19. <https://doi.org/10.3847/PSJ/abedbd>
- Garcia, F., Chambers, F., & Watts, A. (2020). Deep model simulation of polar vortices in gas giant atmospheres. *Monthly Notices of the Royal Astronomical Society*, 499, 4698–4715. <https://doi.org/10.1093/mnras/staa2962>
- Grassi, D., Adriani, A., Moriconi, M. L., Mura, A., Tabataba-Vakili, F., Ingersoll, A., et al. (2018). First estimate of wind fields in the Jupiter polar regions from JIRAM-Juno images. *Journal of Geophysical Research: Planets*, 123, 1511–1524. <https://doi.org/10.1029/2018JE0055510.1029/2018je005555>
- Hansen, C. J., Caplinger, M. A., Ingersoll, A., Ravine, M. A., Jensen, E., Bolton, S., & Orton, G. (2014). JunoCam: Juno's outreach camera. *Space Science Reviews*, 213, 475–506. <http://doi.org/10.1007/s11214-014-0079-x>
- Heimpel, M., Aurnou, J., & Wicht, J. (2005). Simulation of equatorial and high-latitude jets on Jupiter in a deep convection model. *Nature*, 438(7065), 193–196. <https://doi.org/10.1038/nature04208>
- Heimpel, M., Gastine, T., & Wicht, J. (2016). Simulation of deep-seated zonal jets and shallow vortices in gas giant atmospheres. *Nature Geoscience*, 9, 19–23. <https://doi.org/10.1038/ngeo2601>
- Lantz, S., & Fan, Y. (1999). Anelastic magnetohydrodynamic equations for modeling solar and stellar convection zones. *The Astrophysical Journal*, 121, 247–264. <https://doi.org/10.1086/313187>
- Lapeyre, G., & Klein, P. (2006). Dynamics of the upper oceanic layers in terms of surface quasigeostrophy theory. *Journal of Physical Oceanography*, 36, 165–176. <https://doi.org/10.1175/jpo2840.1>
- Li, C., Ingersoll, A. P., Klipfel, A. P., & Brettle, H. (2020). Modeling the stability of polygonal patterns of vortices at the poles of Jupiter as revealed by the Juno spacecraft. *Proceedings of the National Academy of Sciences*, 117(39), 24082–24087. <https://doi.org/10.1073/pnas.2008440117>
- Manneville, J.-B., & Olson, P. (1996). Banded convection in rotating fluid spheres and the circulation of the Jovian atmosphere. *Icarus*, 122(2), 242–250. <https://doi.org/10.1006/icar.1996.0123>
- Moriconi, M. L., Migliorini, A., Altieri, F., Adriani, A., Mura, A., Orton, G., et al. (2020). Turbulence power spectra in regions surrounding Jupiter's south polar cyclones from Juno/JIRAM. *Journal of Geophysical Research: Planets*, 125(7), e2019JE006096. <https://doi.org/10.1029/2019JE006096>
- Reinaud, J. N. (2019). Three-dimensional quasi-geostrophic vortex equilibria with m-fold symmetry. *Journal of Fluid Mechanics*, 863, 32–59. Cambridge University Press. <https://doi.org/10.1017/jfm.2018.989>
- Reinaud, J. N., & Dritschel, D. (2019). The stability and nonlinear evolution of quasi-geostrophic toroidal vortices. *Journal of Fluid Mechanics*, 863, 60–78. <https://doi.org/10.1017/jfm.2018.1013>
- Tabataba-Vakili, F., Rogers, J. H., Eichstädt, G., Orton, G. S., Hansen, C. J., Momary, T. W., et al. (2020). Long-term tracking of circumpolar cyclones on Jupiter from polar observations with JunoCam. *Icarus*, 335, 113405. <https://doi.org/10.1016/j.icarus.2019.113405>
- Yadav, R. K., & Bloxham, J. (2020). Deep rotating convection generates the polar hexagon on Saturn. *Proceedings of the National Academy of Sciences*, 117(25), 13991–13996. <https://doi.org/10.1073/pnas.2000317117>
- Yadav, R. K., Heimpel, M., & Bloxham, J. (2020). Deep convection-driven vortex formation on Jupiter and Saturn. *Science Advances*, 13(46), eabb9298. <https://doi.org/10.1126/sciadv.abb9298>